3-1-2018

Spatial and Temporal Dynamics of Dissolved Oxygen Concentrations and Bioactivity in the Hyporheic Zone

W. Jeffery Reeder
University of Idaho

Annika M. Quick
Boise State University

Tiffany B. Farrell
Boise State University

Shawn G. Benner
Boise State University

Kevin P. Feris
Boise State University

See next page for additional authors

AGU PUBLICATIONS

Water Resources Research

RESEARCH ARTICLE
10.1002/2017WR021388

Key Points:
- Hyporheic hydraulics exert primary control over the functionality of the microbial communities that reside within the hyporheic zone
- The respiration rate, for microbes in the hyporheic zone, is a linear function of the local downwelling velocity
- Reaction rate constants are variable spatially proportionally to dowelling velocity and temporally to carbon availability

Correspondence to:
W. J. Reeder
wjreeder@uidaho.edu

Citation:
Reeder, W. J., Quick, A. M., Farrell, T. B., Benner, S. G., Feris, K. P., & Tonina, D. (2018). Spatial and temporal dynamics of dissolved oxygen concentrations and bioactivity in the hyporheic zone. *Water Resources Research*, *54*, 2112–2128. https://doi.org/10.1002/2017WR021388

Received 24 JUN 2017
Accepted 1 MAR 2018
Accepted article online 8 MAR 2018
Published online 23 MAR 2018

Spatial and Temporal Dynamics of Dissolved Oxygen Concentrations and Bioactivity in the Hyporheic Zone

W. Jeffery Reeder[1], Annika M. Quick[2,3], Tiffany B. Farrell[4], Shawn G. Benner[2], Kevin P. Feris[4], and Daniele Tonina[1]

[1]Department of Civil Engineering, University of Idaho, Boise, ID, USA, [2]Department of Geosciences, Boise State University, Boise, ID, USA, [3]Earth and Planetary Science Department, Harvard University, Cambridge, MA, USA, [4]Department of Biologic Sciences, Boise State University, Boise, ID, USA

Abstract Dissolved oxygen (DO) concentrations and consumption rates are primary indicators of heterotrophic respiration and redox conditions in the hyporheic zone (HZ). Due to the complexity of hyporheic flow and interactions between hyporheic hydraulics and the biogeochemical processes, a detailed, mechanistic, and predictive understanding of the biogeochemical activity in the HZ has not yet been developed. Previous studies of microbial activity in the HZ have treated the metabolic DO consumption rate constant (K_{DO}) as a temporally fixed and spatially homogeneous property that is determined primarily by the concentration of bioavailable carbon. These studies have generally treated bioactivity as temporally steady state, failing to capture the temporal dynamics of a changeable system. We demonstrate that hyporheic hydraulics controls rate constants in a hyporheic system that is relatively abundant in bioavailable carbon, such that K_{DO} is a linear function of the local downwelling flux. We further demonstrate that, for triangular dunes, the downwelling velocities are lognormally distributed, as are the K_{DO} values. By comparing measured and modeled DO profiles, we demonstrate that treating K_{DO} as a function of the downwelling flux yields a significant improvement in the accuracy of predicted DO profiles. Additionally, our results demonstrate the temporal effect of carbon consumption on microbial respiration rates.

Plain Language Summary Dissolved oxygen concentrations and consumption rates are primary indicators of microbial respiration and redox conditions in streambed sediments. The traditional view of streambed microbial activity has treated the metabolic respiration rates as a temporally fixed and spatially homogeneous property that is determined primarily by the concentration of bioavailable carbon. However, our research shows that microbial respiration rates are both spatially and temporally variable. Spatial variability is driven by subsurface hydraulics, such that the respiration rate constant is a linear function of local subsurface flow velocities. For triangular dune type bedforms, subsurface flow velocities are lognormally distributed as are the respiration rate constants. Temporal variability is controlled by the abundance of bioavailable carbon.

1. Introduction

1.1. Hyporheic Flow and DO in the HZ

The bulk chemical activity in riverine environments occurs in the sediments directly adjacent to surface flow (Fischer et al., 2005; Krause et al., 2011; Marzadri et al., 2017; Master et al., 2005; Wuhrmann, 1972). This region of enhanced biochemical activity is termed the hyporheic zone (HZ; Findlay, 1995). Hyporheic exchange, the flow of surface water into and out of the HZ, transports nutrients, pollutants and dissolved oxygen (DO) into the HZ, and transformed products back in the surface flow (Elliott & Brooks, 1997; Krause et al., 2011; Packman et al., 2004; Tonina & Buffington, 2007; Triska et al., 1993a). Hyporheic flow is driven by pressure gradients at the bed surface/surface water interface and can be conceptualized as a series of quasi-discreet and arched flow lines (red lines, Figure 1). Even for simple bed forms, the surface pressure profiles can be quite complex (e.g., blue line, Figure 1). As a result, the interaction between stream bed morphology and surface flow hydraulics influences hyporheic flow velocity and residence times by modulating the pressure gradients at the bed surface (Elliott & Brooks, 1997).

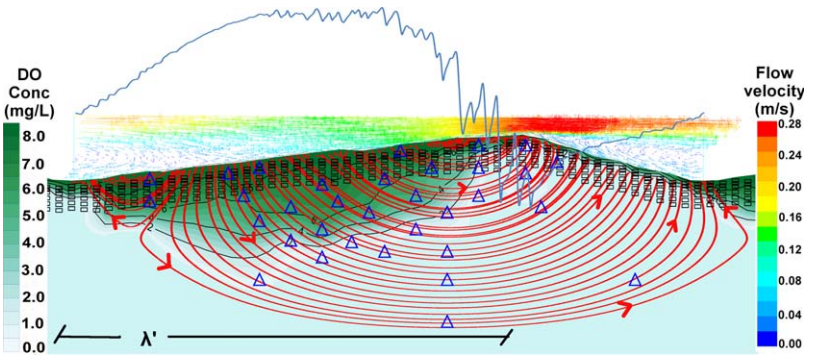

Figure 1. A cross section of a typical dune profile is shown in the center of the figure. Surface flow is shown as multicolored vectors and the bed-surface pressure profile as the blue trace at the top of the figure. Hyporheic flow lines represent as the red traces overlain on the dune and measured and krigged DO profile (green contours). Imbedded DO sensor locations are indicated by the blue triangles and surface probe measurement locations are indicated by the black rectangles. Surface flow is from left to right.

DO is the primary oxidizing agent in most riverine systems and their associated hyporheic zones promoting the metabolic respiration of organic carbon. DO concentrations strongly regulate a suite of processes including nitrogen and carbon cycling, anaerobic respiration (Cooper, 1965; Ocampo et al., 2006; Rutherford et al., 1995a), and the processing of metabolic waste and environmental pollutants (Bott et al., 1984; Master et al., 2005; Triska et al., 1993a, 1993b). Collectively, these hydrochemical processes have a profound effect upon benthic habitat, surface water quality, and the capacity of streams to process biological and environmental compounds (Greig et al., 2007; Tonina & Buffington, 2009). Thus, DO concentration within the HZ, coupled with the associated hydraulic gradients and consumption rates, is primary controls on and indicators of the redox and biochemical state of the HZ (Appelo & Postma, 2010; Cardenas et al., 2008; Chapelle, 1993; Chapelle et al., 1995).

1.2. Spatial Dynamics

With surface waters often near saturation with respect to oxygen, and the subsurface often oxygen limited, the flux of oxygen from the surface to the HZ dictates the magnitude of oxidative processes. The rate of DO consumption is determined by the hyporheic exchange rate and the activity level of the microbial communities in the HZ (Beaulieu et al., 2011; Chapelle, 1993; Henry et al., 2006; Moreno-Vivián et al., 1999; Richardson et al., 2009; Wrage et al., 2001). Common perception holds that the redox and metabolic activity rates of microbial communities are primarily a function of the availability of labile carbon (Harvey et al., 2013; Hunter et al., 1998; Sobczak & Findlay, 2002; Zarnetske et al., 2011a, 2011b), an assumption that is often appropriate when oxygen concentrations are constant. However, during hyporheic influx, DO concentrations decline with respiration and therefore are typically variable. Further, even at the scale of individual bed forms, hyporheic fluxes are also variable. Thus, DO concentrations and fluxes have the potential to influence respiration rate. Empirical studies have reported local zones of increased biologic activity (hot spots). "Hot spot" variations in activity have been attributed to local and random surpluses in high quality, bioavailable carbon (Cleveland et al., 2007; Curiel Yuste et al., 2007; Kayser et al., 2005; Zarnetske et al., 2011a). To the best of our knowledge, no one has attempted to associate variations in hyporheic metabolic activity with a more systemic and ordered cause such as stream hydraulics.

Current practice, in numerical studies of microbially mediated redox dynamics, is to treat the DO consumption rate constant (K_{DO}) as a bulk and relatively fixed material property that is applied homogeneously over the entire domain; see for example, Bardini et al. (2012), Kessler et al. (2012), Marzadri et al. (2010, 2012), Rutherford et al. (1995b), Wriedt and Rode (2006), and Zarnetske et al. (2012). With some notable exceptions (Briggs et al., 2013; González-Pinzón et al., 2014), within the stream ecology community, the notion that rates of microbial aerobic respiration or other redox processes may be a function of the hyporheic flux has not been broadly acknowledged. However, within the microbiology-community it has been, at least by analogy, relatively widely reported. Microbiological reaction and growth rates are commonly studied in chemostatic experiments. A chemostat is a reaction vessel in which the biochemical state of a process can be held in relative stasis. The flux through the chemostat is termed the dilution rate. In chemostatic, microbial

growth experiments, it has been shown that growth rates, respiration rates, nutrient uptake rates, and carbon dioxide release rates all increase linearly with dilution rate (Furukawa et al., 1983; Harrison, 1972; Kayser et al., 2005; Laanbroek et al., 1994; Nobre et al., 2002; PIRT, 1957; Ramirez & Mutharasan, 1990; Rosenberger & Kogut, 1958; Sinclair & Ryder, 1975). In the context of hyporheic flow systems, the chemostatic dilution rate can be seen to be analogous to the downwelling flux along particular flow lines, suggesting that hyporheic DO consumption rates may be spatially variable due to variability in hyporheic fluxes.

1.3. Temporal Dynamics

For hyporheic systems that are subject to episodic nutrient replenishment (e.g., autumnal leaf fall), one would expect that nutrient levels (primarily organic carbon) would change over time, decreasing between replenishment events. Several studies have demonstrated a positive relationship between nutrient concentrations and bioactivity levels (e.g., Argerich et al., 2016; Harvey et al., 2013; Hunter et al., 1998; Sobczak & Findlay, 2002; Suberkropp, 1998; Zarnetske et al., 2011a, 2011b). This idea has also been presented, at least as a theoretical construct, in a number of numerical studies (see e.g., Bardini et al., 2012; Kessler et al., 2012; Marzadri et al., 2010, 2012; Rutherford et al., 1995a; Wriedt & Rode, 2006; Zarnetske et al., 2012). Yet while acknowledging that nutrient concentrations will affect bioactivity levels, these studies have not presented a clear picture of how variable bioactivity in response to changing nutrient supplies will manifest in the HZ. At least as a matter of presentation, these studies have also taken a static, fixed-in-time view of microbial activity in the HZ, thus presenting an incomplete picture of the potential temporal aspects of DO consumption. In general, these studies have been limited by the fact that they did not have access to sufficiently detailed and replicated measurements to resolve DO consumption at the individual flow line level or across biologically meaningful time spans.

One way in which variable bioactivity levels can manifest themselves is the relative apportionment of the HZ into oxic and anoxic domains. Not all environmentally important processes in the HZ are aerobic (Pinay et al., 2009; Zarnetske et al., 2011b) and this partitioning of the HZ into oxic and anoxic domains becomes important when coupled aerobic and anaerobic processes are active. The DO consumption rate defines the extent of the oxic zone and thus the extent of the anoxic zone. By extension, DO consumption rates effectively define to what extent anaerobic metabolic processes occur.

1.4. Research Objectives

Understanding and modeling the dynamics of respiratory processes in the hyporheic zone and the influence on nutrient and pollutant fate requires observations of both biogeochemical changes and physical transport processes. In general, previous field studies have not taken sufficiently detailed and replicated measurements to parse DO consumption to the individual flow line level (Harvey et al., 2013; Naranjo et al., 2015; Nogaro et al., 2013; Pretty et al., 2006) nor have they given a detailed view of the temporal dynamics associated with carbon depletion. When modeling reactive processes in the HZ, researchers have made the explicit assumption that the rate of DO consumption, K_{DO}, is constant within a homogeneous domain (Bardini et al., 2012; Kessler et al., 2012; Marzadri et al., 2010; Rutherford et al., 1995a) and, at least for presentation purposes, made the implicit assumption that K_{DO} is constant over time. Similarly, most work has not attempted to make a strong link between flow hydraulics and DO consumption rates (Boano et al., 2014). In the present study, we address these limitations by taking high-resolution DO measurements, both temporally and spatially, over two long-duration, large-scale flume experiments. Our aims are to (1) elucidate the role of stream hydraulics in DO consumption dynamics and, by extension, hyporheic redox dynamics and (2) separate the roles of mass transfer (hydraulics) and nutrient supplies as related to the reaction rates of dissolved oxygen consumption and (3) to present a more complete picture of DO consumption in the HZ changes as carbon is depleted over time.

2. Methods and Materials

2.1. Experimental Setup

We conducted two sets of experiments, in the large-scale flume (approximately 20 m $\times$ 2 m) at the Center for Ecohydraulics Research Stream Laboratory (Budwig & Goodwin, 2012) at the University of Idaho, Boise. The objective of these experiments was to test the impact of bed morphology, stream hydraulics, and surface water chemistry (reactive nitrogen loading) on DO and nitrogen consumption dynamics and the

impact of those processes on N_2O emissions from streams (Quick et al., 2016). The first flume experiment (Flume 1) ran continuously from August 2013 through December 2013 and the second (Flume 2) ran from February 2015 through June 2015. In both sets of experiments, the flume was divided into three stream channels (30 cm wide $\times$ 60 cm deep $\times$ 15 m long) which were separated by access corridors. Dunes of various sizes were constructed from 90% quarry sand and 10% natural sand collected from the Boise River (Boise, ID). The quarry sand was sieved to remove all fractions above 2.5 mm and washed repeatedly to remove fractions below 0.2 mm. The river sand was sieved in the field to remove fractions above 2.5 mm. The D_{50} of the sand mix was 1.5 mm yielding a hydraulic conductivity of approximately 0.002 m/s. The natural sand provided an inoculum to initiate bacterial communities, which were representative of those that typically reside in streambed sediments. To provide an organic carbon nutrient source, 0.15% by dry weight of finely divided ($<$5 mm) cottonwood leaves were added uniformly to the sand mix. No other nutrient sources were added to the experiment. The water used in the experiment was Boise City water that had been conditioned in the flume's 190,000 L catch basin for 2 months prior to running the experiment. Recirculating flow through the channels (2.1 L/s/channel) was supplied by a submersible pump. Average flow velocity was approximately 0.08 m/s with a mean depth of approximately 7 cm.

In situ DO sensors embedded in the bulk of the dunes and surface probes attached to the flume's robotic instrument cart allowed us to obtain high-density DO measurements throughout the duration of the experimental runs. The 4 mm diameter in situ DO probes were assembled in-house using fiber optic cables and sensor optodes manufactured by PreSens Precision Sensing GmbH, Regensburg, Germany. A typical placement of the in situ DO probes is illustrated by the blue triangles in Figure 1. The probes protruded approximately 10 cm through the channel wall into the bulk of the dunes. The in situ probes were operated on a daily basis for the duration of the experiments. Surface probe measurements were taken at 2 cm longitudinal intervals along the centerline of the bed-surface profiles at depths of 0, 5, 10, 20, 30, and 40 mm (black rectangles, Figure 1) using Clark-type, DO micro sensors (Unisense A/S, Aarhus, Denmark) attached to the flume's robotic instrument cart. Surface probe measurements were taken on approximately two-week intervals. For the present discussion, we will consider three different dune variants. From Flume 1, we will evaluate the response of a 9 cm tall by 1 m long dune, hereafter referred to as the "9 cm dune." The energy slope for the 9 cm dune was 0.002. From Flume 2, we will consider a 9 cm tall by 100 cm long dune and a 9 cm tall by 70 cm long dune, hereafter referenced as "100 cm dune" and "70 cm dune," respectively. The energy slope for the Flume 2 experiments was 0.003. In Flume 2, the 70 cm Dune and the 100 cm Dune were replicated in the three channels. The replicates are designated as Channels A–C.

2.2. Bed-Surface Pressure Profiles and Hyporheic Flow Lines

At the bed form scale, hyporheic flow is driven by local pressure gradients along the bed surface. As illustrated in Figure 1, flow generally enters the dune on the upstream face and exists on the downstream face. This results in a series of quasi-discreet and arched flow lines, with the shortest near the dune peak and the longest entering more proximal to the upstream dune trough and exiting near the downstream trough (red lines, Figure 1). In order to calculate residence times at specific locations within the bed and the flow paths to those locations the total pressure (static plus dynamic pressure) must be known along the entire profile of the bed form. Unfortunately, we did not have the physical capability to measure the bed-surface pressure with sufficient accuracy. Instead, following the approach described by Cardenas and Wilson (2007), we modeled the pressure profiles using ANSYS Fluent CFD (ANSYS Inc., Canonsburg, PA). ANSYS CFD provides a numerical solution to the Reynolds-averaged, Navier Stokes surface flow equations. Our models, which were constructed between 65,000 and 95,000 triangular elements, used a k-ω turbulence closure with a low-Reynolds-number correction. Physical inputs into the models included measured bed surface a water surface profiles and surface flow velocity. The inlets and outlets of the surface flow models were treated as periodic boundaries with the periodic pressure gradient defined by the energy slope of the water surface. The water surface was modeled as a symmetry boundary and the bed surface as a no-slip wall boundary. Residual error for continuity, x-velocity, y-velocity, k, and ω was set to less than 1×10^{-6} for convergence. Figure 1 shows, without scaling, a typical bed-surface pressure profile (jagged blue line at the top of the figure) and surface water velocity vectors (multicolored vectors in the center of the figure) of a typical modeled surface flow. The overall CFD modeling approach was validated against the pressure measurements provided by Fehlman (1985; Figure 2a). The excellent agreement of the simulated bed-pressures to the measured values, over a broad range of discharges and energy head, gave us a high degree of confidence

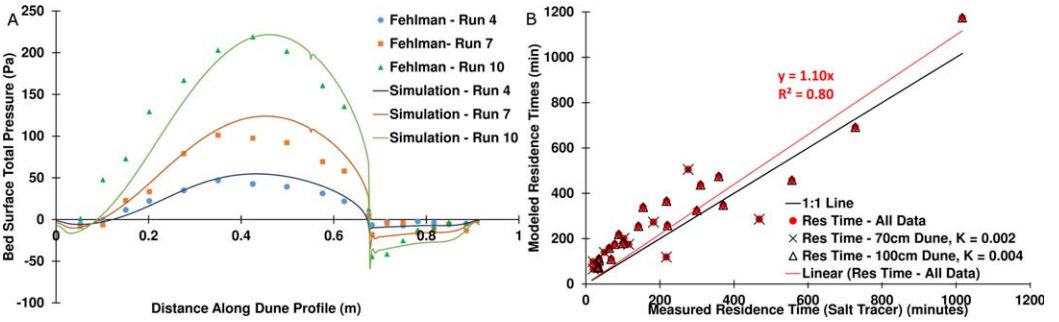

Figure 2. (a) The modeling technique used to create the bed-surface pressure profiles was validated against the data of Fehlman (1985). The discreet points represent the measured values provided by Fehlman. The continuous lines are the modeled simulations. The ΔP for Run 4 was 23Pa/m, 54Pa/m for Run 7 and 98Pa/m for Run10. Discharges per meter of bed width for the same runs were 65, 98, and 130 kg/s, respectively. Flow depth at the dune crest was 0.15 m for all runs. (b) The residence times derived from the calculated flow lines were validated with physical measurements using salt tracer tests.

that our modeling approach was robust, accurate and not overly sensitive to the applied boundary conditions.

Hyporheic flow lines and the associated residence times (τ) were calculated using the model of Marzadri et al. (2010) and GMS ModFlow. The Marzadri model supplies a semi-analytical solution to the groundwater flow equations while ModFlow provides a numerical solution. The two modeling approaches were used as a cross check and to take advantage of the visual presentation of the GMS ModFlow output. The red lines overlain on the dune cross section and DO concentration profile in Figure 1 are typical of flow line profiles used for analysis in this experiment. The data stream for each flow line is a series of X, Y positions coupled with a calculated residence time, τ, for a parcel of water to reach each position along the flow line. To validate the calculated residence times, at the end of Flume 2, we removed the DO probes from several of the in situ measurement locations (blue triangles, Figure 1) and replaced them with electrical conductivity (EC) sensors that were designed in-house and assembled by Rapid Creek Research (Boise, ID). The sensors featured a cylindrical stainless steel sleeve anode (15 cm by 4 mm) and a platinum wire cathode (~0.5 mm diameter). We injected a concentrated salt solution into the head box of the flume as a continuous stream for approximately 30 min to bring the surface water concentration up to approximately 100 m*M*/L. EC was logged every 5 min for each of the sensors using Model CR1000 data loggers (Campbell Scientific, Logan, UT). Residence times were computed from breakthrough curves generated from EC data at 9 locations in a 70 cm dune and 20 locations in a 100 cm dune. The correlation of measured to modeled residence times is shown in Figure 2b.

2.3. Calculating DO Consumption Rate Constants

We used two separate methods to calculate DO consumption rate constants (K_{DO}) for each of the flow lines. In the primary methodology, we first created DO concentration profiles for each dune on each evaluation date using all the surface and in situ DO probe data for that dune and date. Using the mapping software Surfer® Version 10 (Golden Software, Inc., Golden CO) the measured DO data were krigged and gridded to create DO concentration maps (see the green shaded concentration profiles in Figures 1 and 6). These DO concentration profiles comprise a regular array of X-Y locations and a DO concentration at each location. We then mapped the appropriate flow lines (red lines, Figure 1) onto all the DO concentration profiles. The flow line traces comprise a series of X-Y locations and a residence time at each location. From the two overlain data sets, we extracted, for each flow line a DO consumption profile. That is, a data stream that is the mated pair of residence time and the DO concentration (τ, [DO]) for each flow line (Figure 3). To simulate first order reaction mechanics, an exponential fit was calculated for each of the DO consumption profiles. In this approach, the residence time for any position along a particular flow line is a function of all of the prior positions along that flow line. The DO concentrations, at any given point, are interpolated from nearby measured values.

The second method was used to insure that the form of the K_{DO} response was not simply an artifact of the data structure in the krigged DO profiles and to isolate the activity of the sediments along the surface profile. In the second approach, K_{DO} values for the sediments along the surface profile were calculated using only the surface probe data. Residence times to each of the measurement positions (black rectangles,

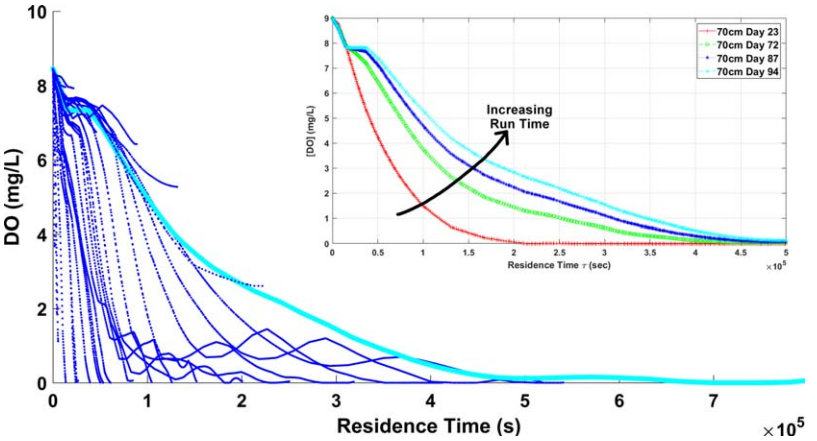

Figure 3. DO concentration versus residence time (τ) for each of the individual flow lines (blue traces) in a single dune (Channel A, 70 cm, Day 94). Note the range of slopes exhibited by the individual traces, indicating a significant range of DO consumption rate constants (K_{DO}). The inset tracks the behavior of a single flow line (aqua trace in the main figure) over 2 month's run time.

Figure 1) along the dune surface profile were calculated individually by back-particle tracking. Each set of six vertically aligned measurement points was treated as a functional flow line and an exponential fit was calculated for each of those vertically aligned sets. In this method, all of the DO concentrations used in the K_{DO} calculations are from direct measurement (no interpolation).

For both methods, we assumed that the reaction mechanics of DO consumption were first order. For first-order reactions, the decay is exponential and the reaction equation takes the form:

$$[\mathrm{DO}]_\tau = DO_0 \; e^{-K_{DO}\tau} \tag{1}$$

where $[DO]_\tau$ is the DO concentration at residence time τ along a flow line, K_{DO} is the first-order reaction rate constant, τ is the residence time of a parcel of water traveling along a flow line, and DO_0 is the surface water DO concentration. Exponential (first-order) curves were fit to all (n = 2,008) of the flow line (τ, DO) data streams. Approximately 95% of the flow lines had an R^2 of 0.8 of higher.

2.4. Data Presentation

Using the procedure previously described we calculated the DO consumption rate constants (K_{DO}) for all of the modeled flow lines for the 9, 70, and 100 cm dunes at several dates through the two experimental runs. Longitudinal spacing of the modeled flow lines, along the bed surface, was roughly 2 cm. To describe the spatial distribution of K_{DO} values, the locations of the calculated values are assigned to the x-locations of the entry points of the flow lines into the HZ. To represent different bed geometries on the same scale, we plot the K_{DO} as a function of X*, which is the downwelling location (x) normalized by the length (λ') of the upstream face of the dune ($X^* = x/\lambda'$). The extent of λ' is indicated at the bottom of Figure 1. Note that for all of the graphs that employ calculated K_{DO} values or calculated downwelling fluxes (q_{dw}) values, for presentation purposes the presented values have been multiplied by a factor of 1×10^5. For example, if a value of K_{DO} or q_{dw} of 2.5 is read from a graph, the associated physical value is 2.5×10^{-5}.

3. Results and Discussion

3.1. Spatial Dynamics

At the beginning of the project and in agreement with current understanding of reactive solute transport dynamics, our expectation was that all of the flow lines would exhibit essentially the same rate of DO consumption with residence time. If this were the case, the DO consumption profiles (τ versus [DO]) for each of individual flow lines would map onto a single, common profile. Short flow lines would occupy a relatively short segment of that profile with the longest flow lines defining the full extent of the common profile. Surprisingly, we do not observe the same rates of oxygen consumption with residence time. Specifically, we observe higher rates on flow paths with higher velocities, suggesting the rate is a function of O_2 flux. When

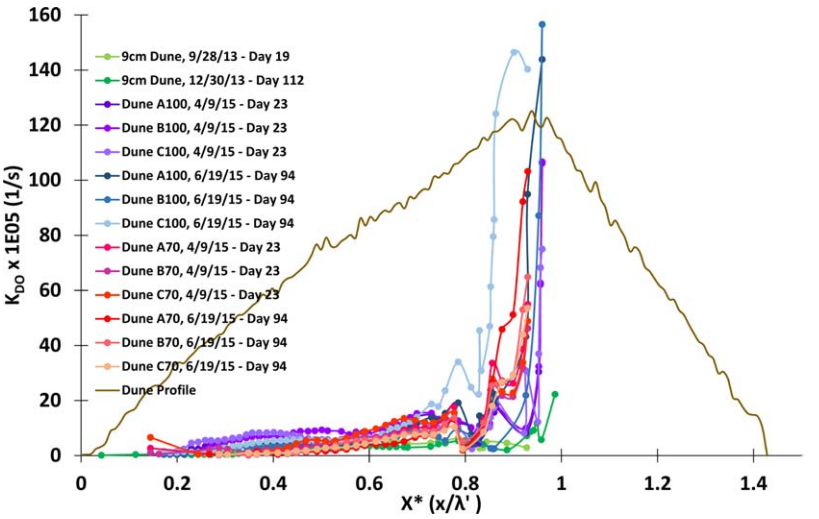

Figure 4. K_{DO} profiles for all of the dunes considered in this experiment early and late in the runs for Flume 1 and Flume 2. The form and magnitude of the KDO profiles is consistent across experiments (Flume 1 and Flume 2), dune geometries, dune relicates and rune time. Note: Physical values represented on the vertical axis have been multiplied by 1E05, i.e., a graph reading of "5" corresponds to a physical value of 5E-05.

evaluated at the scale of individual flow lines (primary method, section 2.3), microbial respiration exhibits a broad range of DO consumption profiles (blue traces, Figure 3) and, thus, a broad range of DO consumption rates. The profiles presented in Figure 3 are for a single dune at one point in time (Channel A, 70 cm dune, 19 June 2015, Day 94) but this behavior is characteristic of all of the dunes at all measurement points over the durations of both of the experiments.

K_{DO} values were calculated for all of the flow lines for the various dunes and at several points in time across the run time of the two experiments. Each flow line K_{DO} value is represented by the individual dot on the various K_{DO} profiles (Figure 4). The K_{DO}-dots are located at the X* coordinate of the entry point of the associated flow line into the HZ. A dune profile is included in the figure for visual reference. The behavior of these profiles is consistent across dune replicates (Channels A–C) of the 70 and 100 cm dunes and consistent across time, though not constant. While it is difficult to discern in Figure 4, there is a temporal trend to the K_{DO} profiles. This will be discussed in section 3.2. It is important to note the shape of the K_{DO} profiles. For all of the traces, the K_{DO} values are quite low near the trough of the dune and rise gently moving toward the crest. In the middle of the downwelling area, the K_{DO} values are relatively constant and then rise sharply at the crest of the dune. The general observation is that K_{DO} values are low where the downwelling flux (velocity) is low and high in areas of high downwelling velocity. Importantly, K_{DO} values are calculated and expressed as a function of residence time (τ). The DO consumption rates are not based upon mass or the size of a control volume. Therefore, the variation in the reported K_{DO} values is an indication that the activity levels of the microbial community are differentiated between flow lines and not a simple linear scaling of the mass flux.

The K_{DO} profiles generated by the two calculation methods (section 2.3) are consistent in both form and magnitude (Figure 5). The DO consumption rate constants calculated from direct measurement of DO concentrations in just the top 4 cm of the dune surface (secondary method) yields the same response as the krigged measurements interpolated throughout the bulk of the dune (primary method). This indicates that (1) the form of the DO consumption profile is not a function of the data structure (i.e., an artifact of krigging) but rather due to variations in biologic activity levels and (2) that aerobic respiration starts at the bed-surface/water interface and continues consistently along the flow lines until DO is depleted or until the flow line exits the dune. It is interesting to note that near the crest ($X^* > 0.6$) the bulk flow lines (primary method) exhibit consistently higher values of K_{DO} than the surface profile sediments (secondary method). This may be an indication of decreased bioactivity in the surface sediments, possibly due to carbon depletion in the surface sediments relative to the bulk.

The consistent and persistent form of the K_{DO} profiles suggests that an overarching and steady process is driving the K_{DO} behavior and that the observed values for the downwelling flux and/or aerobic respiration

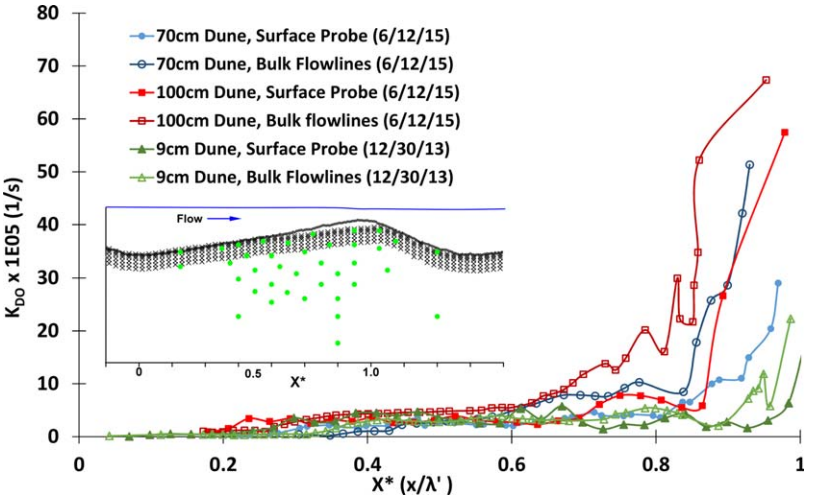

Figure 5. In both flume experiments, DO consumption rate constants (K_{DO}) were calculated using two separate methods (section 2.3). The primary method (open markers) used all of the krigged data and KDO was calculated for the full extent of the flow line. The seconary method (filled markers) used only the directly measured DO values from the surface probe measurement locations (black rectangles, Figure 1). K_{DO} was calculated for only the first 4 cm of the flow line. Surface probe measurements were taken along the surface profile at approximately 2 cm intervals at depths of 0, 0.5, 1, 2, 3, and 4 cm. Only downwelling locations are represented in these data. Note: Physical values represented on the vertical axis have been multiplied by 1E05, i.e., a graph reading of "5" corresponds to a physical value of 5E-05.

rate would adhere to a recognizable probability distribution. The model of Marzadri et al. (2010) provides a value of the downwelling flux ($q_{dw} = V_{dw} \times \rho$) at each flow line entry point. We tested the downwelling fluxes against a variety of distributions and found that, for all of the bed form configurations investigated, the calculated q_{dw} values conform to a lognormal distribution (Figure 6a). Figure 6b shows the quality of fit for q_{dw}. We similarly tested the K_{DO} data sets and found that for all configurations and on all evaluation dates, the K_{DO} values conform to a lognormal distribution (Figure 6c). The quality of fit for the K_{DO} distribution is shown in Figure 6d. The quality of fit for the flux and K_{DO} data, to a lognormal distribution, was evaluated using the Kolmogorov-Smirnoff test. All data sets passed the acceptance criteria.

The lognormal distribution of downwelling velocities for triangular dunes is a natural property of the interaction between the stream hydraulics and the dune morphology (Wörman et al., 2002). Previous studies have noted, without causal explanation, that hyporheic residence times are lognormally distributed (Marzadri et al., 2010; Wörman et al., 2002). We can now propose that, at least for dune-type bed forms, the reason for the lognormal distribution of hyporheic residence times is that downwelling velocities are lognormally distributed. The lognormal distribution of K_{DO} values is a result of the fact that biological activity levels are linearly proportional to the flux (Figure 7). Whether or not the downwelling velocities of other bed forms will adhere to a lognormal distribution is unknown (expect for pool-riffle which seems to be also lognormal; Tonina & Buffington, 2011). Nonetheless, we can propose with some confidence that, regardless of the bed morphology and given a relative abundance of bioavailable carbon, downwelling fluxes will have strong influence over the levels of biological activity. This suggests that hyporheic hydraulics effectively controls biogeochemical processes, not just nutrient availability.

In essence, what we are proposing is a move from a concentration-based reaction rate model to a flux based reaction rate model. The traditional view of biochemical reactions is that reaction rates are controlled by the ambient concentrations of the chemical resources and the transport rate (diffusion) of those resources to the microbes (King et al., 2014). In this view, even in a system experiencing a flux, the reaction rates will be controlled by the concentrations around the static boundary layer of fluid surrounding the microbes and the diffusion rate across the boundary layer. Reaction rates are perceived to be independent of the flux. However, our results indicate that the rate at which resources are delivered to the local environment (flux) does have an impact on biochemical reaction rates. The physical explanation for this is not known but we can speculate that is related to availability and transport of resources. Fluxes certainly account for availability but not for transport of resources to the cells. It appears that the local flow velocity is having an

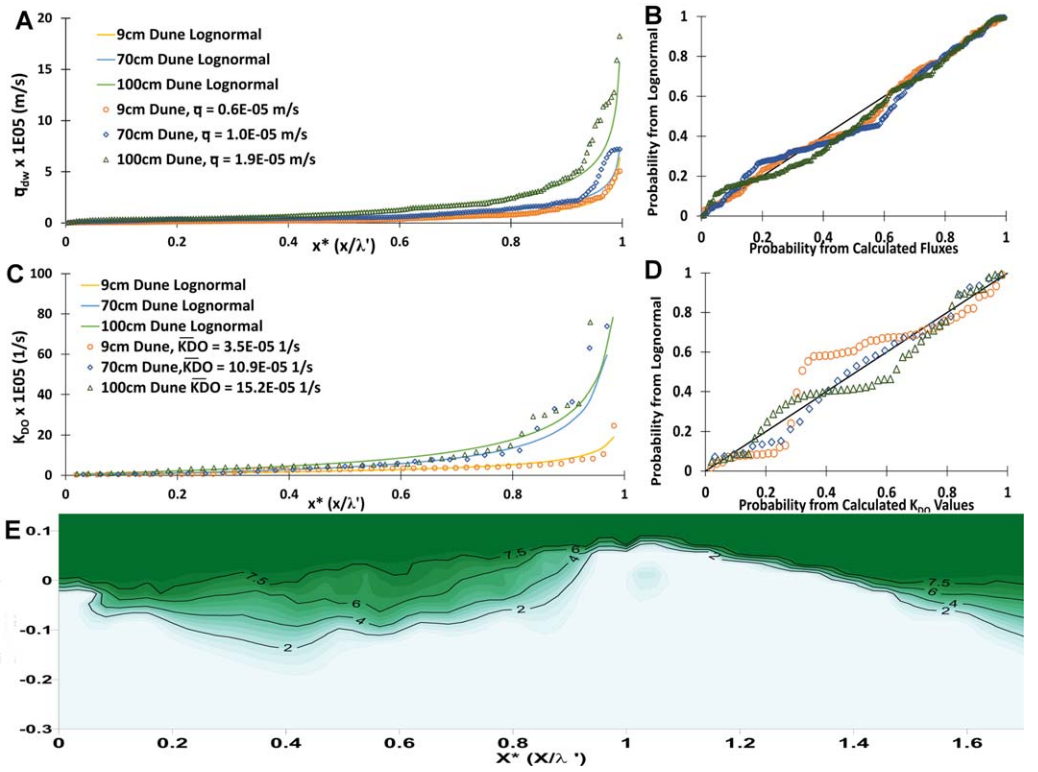

Figure 6. The values of the downwelling flux ($V_{dw} \times \rho$) and K_{DO}, for individual flow lines, are lognormally distributed across the downwelling area. (a) The lognormally distributed downwelling fluxes for the 9, 100, and 70 cm dunes. The open markers are the calculated q_{dw} values for the individual flow lines and the solid lines are the lognormal profile calculated from the mean and standard deviations of the log-transformed data. (b) The quality of the lognormal fit with calculated q_{dw} versus modeled values tightly grouped around the 1:1 line. Similarly, the calculated and lognormal modeled values of K_{DO} are shown in (c) and (d). For spatial context, the lognormal profiles (charts on the left) are spatially aligned with downwelling area of a representative dune, shown by the DO profile at the bottom of the figure (e). Note: For panels A and C the physical values represented on the vertical axis have been multiplied by 1E05, i.e., a graph reading of "5" corresponds to a physical value of 5E-05.

impact upon the effective diffusion rate across the boundary layer. There is some support for this observation in the literature. Stewart (2012) showed that Sherwood number for external mass transfer to cells in a biofilm had a power law relationship to the Reynolds number of flow over the biofilm (i.e., as flow velocity increases so too does mass transfer). This relationship may be due to morphological responses of biofilms to flow velocities. Slow laminar flows have been shown to promote thick, smooth biofilm structures that tend to act as a diffusion barrier. In contrast, higher velocity and turbulent flows tend to promote thinner, highly textured biofilms (Hödl et al., 2014; Stewart, 2003, 2012; Stewart et al., 2009). It is likely that these thinner, textured films will have stronger interactions with the surrounding advective flow than the thicker smooth films, increasing their opportunity to bring in oxygen and nutrients while efficiently disposing waste products. Validation of this hypothesis will be the subject of future research.

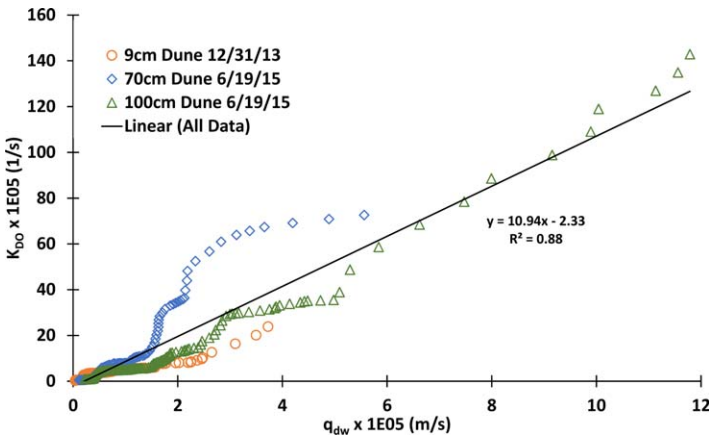

Figure 7. Flow line level K_{DO} values are plotted against the associated q_{dw}. The fit line shown here is for all of the data, the relationship is linear with an r^2 of 88%.

3.2. Temporal Dynamics

The spatial and temporal responses of DO consumption are driven by different mechanisms. The spatial variation is driven by the flux. In contrast, the temporal variability is driven by the availability of carbon. For a system that is characterized by episodic carbon replenishment, after a replenishment event our data shows that the rate of DO consumption changes continuously and progressively over time. Specifically, unless

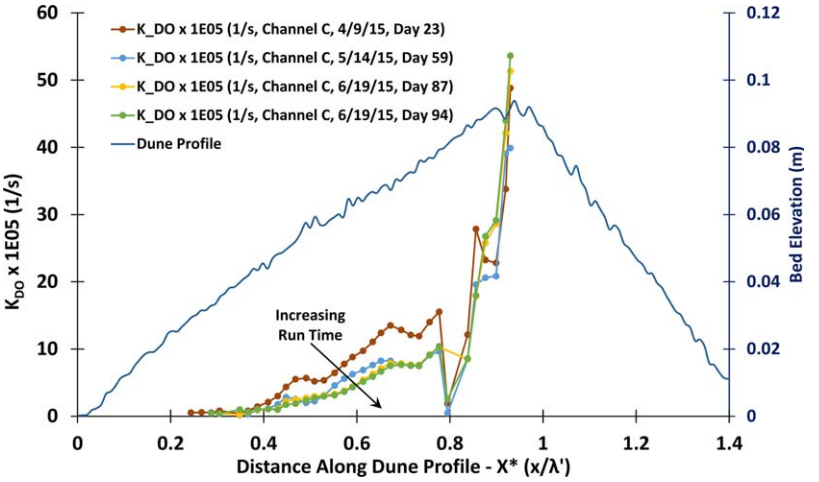

Figure 8. The temporal changes in flow line K_{DO} is manifest across the downwelling area. Here we see the steady and consistent decrease in K_{DO} values over a 2 month time period. Note: Physical values represented on the vertical axis have been multiplied by 1E05, i.e., a graph reading of "5" corresponds to a physical value of 5E-05.

organic carbon is continuously replenished to the hyporheic environment, the rate of metabolic activity, as measured by DO consumption rate, decreases as bioavailable carbon is depleted. This can be illustrated by isolating a single flow line and tracking its response over time as carbon is depleted. Additionally, by focusing on a single flow line, we eliminate any spatial variability from the DO consumption response. The inset graph in Figure 3 show the progression of the DO consumption response over approximately 2 month's run time for the flow line represented by the aqua-colored trace in the main figure. This particular flow line entered the HZ in the middle of the stoss face of the 70 cm dune in Channel A and exited the lee face of the same dune. The red, left-most line in the inset graph shows the DO consumption profile at about 5 weeks into the experimental run. The aqua, right-most line shows the DO consumption profile approximately 2 months later. The green and blue lines are, progressively, intermediate profiles. The aqua trace is at the same point in time in both graphs. Over time, the rate of DO consumption is decreasing as witnessed by the decreasing slope of the DO consumption profiles. Over this span in time the measured K_{DO} values ranged from 1.6×10^{-5} s^{-1} on 19 April 2015 (Day 33) to 0.6×10^{-5} s^{-1} on 19 June 2015 (Day 91), decreasing by a factor of 2.75. Additionally, as run time increases, the overall residence time needed for the flow line to reach a fully anoxic state ([DO] = 0) increases, further illustrating the diminishing rate of oxygen consumption.

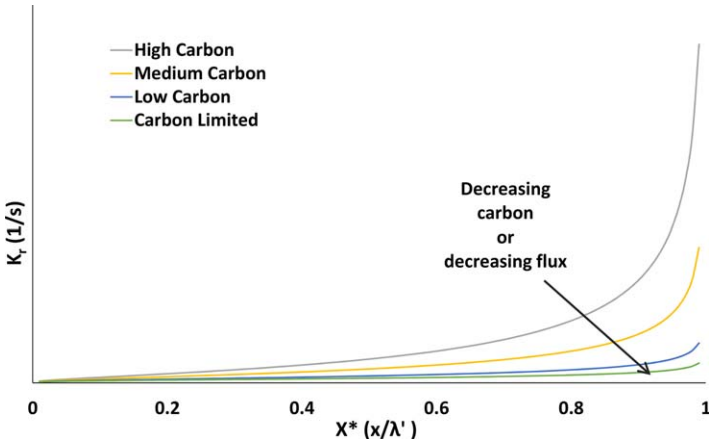

Figure 9. As carbon is depleted from a system, the overall biological reaction rate is expected to decrease and at some limiting carbon concentration the impact of the downwelling flux will be minimized. Similarly, for any given bed form morphology and carbon concentration, the strength of the lognormal relationship will decrease as the flux decreases.

This trend of generally decreasing DO consumption rates can also be observed in the overall K_{DO} profiles for the individual dunes. Figure 8 shows the K_{DO} profiles at four different dates for the Channel C, 70 cm dune. All of the profiles have the characteristic spatial profile in which K_{DO} rises slowly along the stoss face of the dune and then terminates in a sharp rise at the crest of the dune. Superimposed on this spatial profile is a temporally decreasing trend in DO consumption rates that is consistent and exhibited across the dune profile. It is particularly prominent in the middle of the stoss face of the dune in the center of the downwelling area. It is interesting to note that this transition is not so readily apparent in the crest region. This is a bit counterintuitive. It would seem that this area should exhibit the largest delta in K_{DO} values since, due to the significantly higher fluxes in that area, the rate of carbon depletion should be highest in that area. The crest had some slight bed turnover and sediment movement. It may be the case that there was some local carbon replenishment occurring due to particle transport and modest bed mobility at the crest (Drummond et al., 2014; Harvey et al., 2012).

At some lower limit of carbon availability, it is expected that the variability in K_{DO} in response to downwelling flux distribution would be

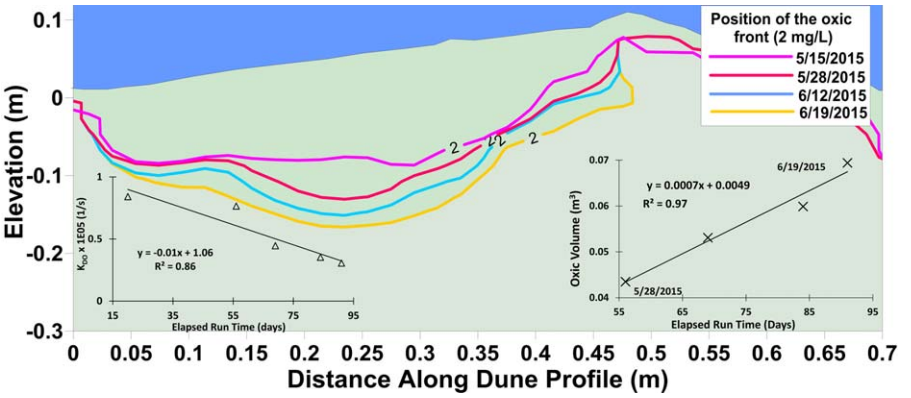

Figure 10. As the supply of labile carbon is depleted (first near the surface of the downwelling area), the DO consumption rate constant, K_{DO}, decreases causing the plume of DO to extend further into the HZ. The rate of expansion for the volume of the oxic plume is, over the time period of this experiment, linear (see right inset). Similarly, K_{DO} decreases linearly (left inset).

diminished or eliminated because of extremely low levels of bioactivity in a truly carbon limited system (Figure 9). Stated another way, if a constant value of K_{DO} is observed across a system, this implies that the system is substantially carbon deficient. For high-mountain, headwater streams where organic carbon supplies are relatively scarce, the value of K_{DO} should be relatively constant. Streams below the tree line and in agricultural and urban environs are not likely to be carbon limited and thus, in these streams, the value of K_{DO} should be a function of the downwelling velocity. This may result in lognormally distributed reaction rates, assuming the lognormal distribution of downwelling fluxes applies generally.

The supply of bioavailable carbon was fixed at the beginning of the run and not replenished at any point during the experimental run. The flow hydraulics and bed morphology were held as relatively fixed quantities for the duration of the experiments (~15 weeks) as was surface water temperature. Thus, the observed decrease in K_{DO} must be linked to internal changes in the hyporheic environment as opposed to some external forcing. The only free variables here are reactive carbon concentration and the composition and quantities of the microbial communities. Barring some disruptive event, the microbial communities will adapt their numbers and activity to match availability of resources—in this case DO and organic carbon. Except for any lithoautotrophic activity, organic carbon reactivity/availability should only decrease with time. Metabolic depletion of labile carbon would be first observed near the surface of the bed form and move progressively downward into the HZ. The net effects of decreasing carbon are the observed decrease in bioactivity (K_{DO}; Figure 8) and deeper penetration of DO into the HZ (Figure 10). Because of this progressive depletion of labile carbon, the extent of the DO plume expands over time. For this system and for the period captured by these data, the volume of the DO plume increased linearly with time and, similarly, the mean K_{DO} values for the same dune decreased linearly with time. Evaluated over a longer period it is possible that the rate of change is actually exponential. Given sufficient runtime and lacking nutrient replenishment, the volume of the oxic plume would be expected to occupy the entire volume encompassed by the hyporheic flow lines. Based upon the extent of the flow lines and the linear expansion rate, the 70 cm dune analyzed in Figure 10 would take approximately 240 days to become fully oxic. Along with the expanding extent of the oxic volume is an associated decrease in the anoxic volume and with that a decrease in the residence time available for anaerobic processes.

3.3. Effects of Spatial Dynamics on DO Consumption Modeling

Most reactive solute transport models use a procedure similar to the one that we described to generate bed-surface pressure profiles and, as a result, apply hyporheic fluxes that correctly represent those in the associated physical system. However, applying a single value of K_{DO} to describe the reaction dynamics for the entire volume of the modeled bed form may result in a misrepresentation of the morphology and extent of the DO plume. More importantly, it is likely to result in a misrepresentation of the functionality of the microbial communities.

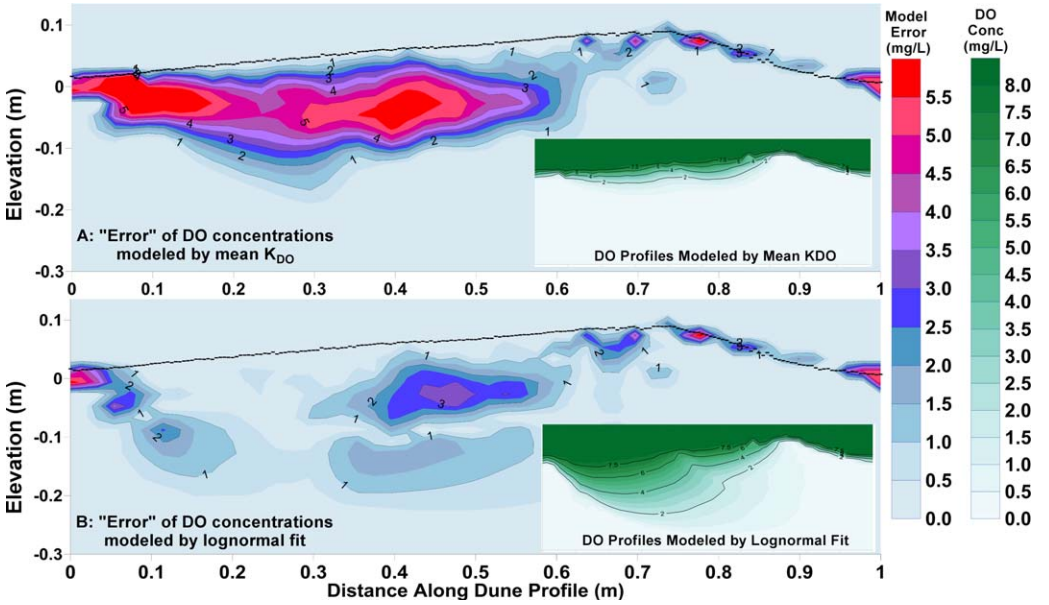

Figure 11. (a) The top chart is the error for a DO consumption model that employs a single value of K_{DO} fro the entire domain. The K_{DO} value used in this model was the mean of all of the individual flow line K_{DO} values calculated from the measured and krigged data for this dune. The modeled DO concentration profile is shown in Figure 11a inset. The error for the model generated by assigning unique K_{DO} values to the individual flow lines per the lognormal distribution is show in (b). Error is calculated as the difference between the measured (krigged, Figures 1 and 6) and modeled profiles.

The net effect of applying a single value for K_{DO} for the entire domain is shown in Figure 11. This figure presents the modeling error associated with employing a single value of K_{DO} (Figure 11a) and a lognormally distributed K_{DO} (Figure 11b). The results presented here are for the Channel A, 100 cm dune on 19 June 2015 but are typical of the other dunes and dates. Error is calculated as the difference between the krigged DO concentrations (green profiles, Figures 1 and 6) and the modeled concentrations (shown as insets on plots a and b).

The K_{DO} value used in the single-value model is the mean of the flow lines for that dune on that date. Other values are certainly possible but the mean of the flow line values is likely to be representative of what might be determined from point measurements in a field study. The K_{DO} values used for the lognormally distributed model were generated from the lognormal function using the mean (same as the single-value model) and the standard deviation of the K_{DO} values for that dune. Visually, the difference between the two models (insets, Figure 11) is quite striking. The extent and morphology of the DO plume in the model that uses the lognormally distributed K_{DO} values matches the measured profile much more closely than the single-valued model. More quantitatively, the difference (error) between the krigged profile and the modeled profiles is shown in Figure 11a and 11b. The model using a single value for K_{DO} (Figure 11a) has significantly higher errors than the distributed model with the largest errors in the heart of the oxic zone. The magnitude of some of these errors approaches the concentration of DO in the surface water. The errors exhibited by the lognormally distributed model, while significant at some locations, are substantially smaller in magnitude and extent than for the single-valued model. In the heart of the HZ, the errors produced by the lognormal model are quite low. The lognormal distribution more accurately reproduces the DO concentration profiles and the true shape and extent of the DO plume.

If the only point of interest for constructing a DO consumption model were to describe the DO consumption capacity of the dune, for the dunes in our experiments the net result difference between the two approaches would be small. In that physical context, DO is completely consumed along the substantial majority of the flow lines before they exit the HZ and, thus, the two models would have roughly the same DO consumption capacity. If, however, anaerobic processes are of interest (e.g., anaerobic denitrification), the constant K_{DO} model will likely allocate an incorrect amount of residence time to those processes, significantly misrepresenting the capacity for those processes and the potential for them to be carried to

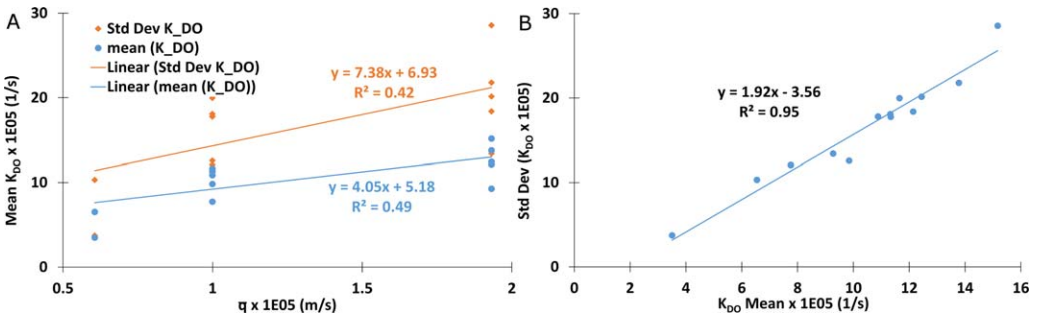

Figure 12. (a) A plot of the mean value for each the individual KDO profiles (as in Figure 4) versus the associated $\bar{q}$ yields a modest linear relationship. Similarly, the standard deviations of the KDO values in those profiles also yield a linear relationship to $\bar{q}$. The data presented here are for the 9 cm Dune ($\bar{q} = 0.606$ on Days 72 and 112), 100 cm Dune ($\bar{q} = 0.99$ on Days 59, 72, 76, 87, and 94), and 70 cm Dune ($\bar{q} = 1.93$ on Days 59, 72, 76, 87, and 94). (b) Over the range of values described by the present experiment, the standard deviations of the various KDO distributions have a linear relationship with the means of those distributions. Note: Physical values represented on the vertical axis have been multiplied by 1E05, i.e., a graph reading of "5" corresponds to a physical value of 5E-05.

completion. In this particular case, the constant K_{DO} model allocates significantly more time for anaerobic processes than is actually available in the physical system. Further, as time goes forward and carbon is consumed, there will come a point at which a significant portion of the flow lines will not consume all of the dissolved oxygen that is being transported. In these later stages, some of the flow lines will exit the HZ still in a semioxic state. The single-value model will likely do a poor job of representing this scenario.

3.4. Using Field Data to Construct Lognormal Distributions

All of this raises a problem for simulations that are based upon field-gathered data: how to define properly the lognormal distribution of K_{DO} values. Fortunately, the lognormal distribution is fully defined by the log-mean and log-standard deviation and is expressed as

$$f(X^*|\mu,\ \sigma)\ \frac{1}{X^*\sigma\sqrt{2\pi}}e^{\left\{\frac{-(\ln x-\mu)^2}{2\sigma^2}\right\}};\ X^*>0 \tag{2}$$

where μ is the log-mean and σ is the log-standard deviation. Thus, if enough measurements are taken to make a reasonable estimate of the mean and standard deviation (K_{DO} or q_{dw}), then the lognormal distribution can be constructed from those values. Alternatively, at least within the constraints of our experimental system, we found some relationships that might be useful in estimating the parameters needed to construct the lognormal distribution. There is a modest linear relationship between the mean downwelling flux of a bed form and the mean K_{DO} and the standard deviation (Figure 12a). In addition, the mean and standard deviation of the K_{DO} values appear to be linearly related, i.e., the standard deviation is proportional to the mean (Figure 12b). Whether or not these relationships hold in a more general sense is unknown but, at a minimum, the trends are instructive of the basic relationships.

3.5. Implications

Our results suggest that two mechanisms exert primary control over biochemical activity in the HZ: the magnitude of the downwelling flux (downwelling velocity) and the concentration of bioavailable carbon. The distribution of the downwelling fluxes is the primary driver of the spatial distribution of K_{DO} values and carbon concentrations are the primary driver of temporal distribution of K_{DO} values. The proportionality of K_{DO} to the downwelling velocity suggests that the crest of a dune and, indeed, any area of relatively high downwelling flux will be a "hot spot" of biochemical activity. These hot spots are zones of high consumption/production capacity and are, on a volume basis, likely to contribute disproportionally to the process capacity of the streambed. We expect that the dependency of K_{DO} values on fluxes can be scaled from the flow line regime to the bed form or reach scale. It seems certain that, within a given reach, features such as step-pools, pool-riffle sequences and woody debris obstructions that cause large pressure gradients and high downwelling fluxes will have significantly higher redox rates, i.e., aerobic respiration, than features such as small dunes and ripples. Extending this idea further, we expect that other respiratory and biologically mediated redox processes in the HZ to follow the same pattern as DO consumption. We expect the

rate constants for the chemical transformations in processes such as the nitrification/denitrification sequence to be linearly proportional to the local flux and, thus, lognormally distributed over the extent of the downwelling area(s) in the case of dune-like bed forms. This is an untested hypothesis that would need to be validated through physical experimentation.

The temporal and spatial trends in DO consumption rates suggest that researchers engaged in field studies need to be cognizant of the temporal and spatial nutrient regime of the study area as well as the hydraulic context and complexity of that area. These trends in bioactivity also add a new dimension to how we interpret field data. For instance, it has been observed that hyporheic activity decreases as the size of rivers increases (Marzadri et al., 2017). This has been previously attributed, at least partially, to decreased hyporheic flux in large rivers, which is due to low hydraulic conductivity of the streambeds and the relatively flat bed morphology of those rivers. Now we can demonstrate that, in addition to these factors, the lower hyporheic activity in large, flatbed streams is also due to lower specific reaction rates in the HZ because of the lower downwelling velocities.

4. Conclusions

In hyporheic systems, aerobic respiration is generally limited by dissolved oxygen (DO) availability. Bed morphology and its interaction with stream hydraulics exert primary control over the delivery of DO and, by extension, over the functionality of microbial communities that reside within the hyporheic zone (HZ). The complex pressure profile that exists even across simple bed forms causes a broad range of downwelling velocities and fluxes and these widely varying downwelling fluxes define the local availability of DO in the HZ. At the flow line scale, we show that hyporheic hydraulics regulates the rate of DO consumption such that DO consumption rate constants are not only directly proportional to DO concentration but rather are a linear function of the velocities of the local downwelling fluxes. This linear relationship between levels of bioactivity and the downwelling fluxes cause the values exhibited by K_{DO} to be spatially distributed as the downwelling velocities across the extent of a bed form. At least within the context of triangular dune morphologies, downwelling velocities are lognormally distributed and, because of the linear relationship between aerobic respiration rates and downwelling velocities, the values of K_{DO} are lognormally distributed. For triangular dunes and presumably other bed forms, the full distribution of K_{DO} values can be generated from the K_{DO} mean and variance, which we found to be linearly related to the mean. The range of K_{DO} values exhibited by a single bed form at a given point in time can be substantial and in our experiments spanned significantly more than an order of magnitude.

In hyporheic systems that are characterized by nutrient replenishment, which is primarily episodic (e.g., autumnal leaf fall), the spatially distributed DO consumption rates change over time. Specifically, between replenishment events and after microbial communities are well established, the rate of DO consumption decreases, presumably as carbon availability decreases. Within the constraints of the period in which the available carbon is above a minimum threshold, the impact of the surface hydraulics will persist in the K_{DO} distribution. However, as the most readily available organic carbon is consumed (first near the bed surface/water interface), respiration rates will drop and DO will be transported deeper into the HZ. Over time, and lacking either an external source of bioavailable carbon or an alternate electron donor substrate, microbial metabolic activity will slow substantially and the majority of the HZ will be rendered oxic. As the bioavailable carbon falls below a threshold, at which the microbial activity is truly carbon limited, it is expected that the K_{DO} profile will flatten and the stream hydraulics will exert less control over the biologic activity.

The range of K_{DO} values that are expressed even within a single bed form because of the spatial and temporal forcing has significant implications for where and when we measure biogeochemical activity in the HZ and how we interpret those measurements. Observed biochemical hot spots may be more a function of the local downwelling velocity or, for some systems, the time elapsed since the most recent nutrient replenishment event rather than local variations in the nutrient supply. Further, the relationship between downwelling velocity and K_{DO} suggests that we need to consider how we evaluate the biogeochemical processing capacity of individual bed forms and stream reaches. Applying K_{DO}, or other chemical species rate constants, as a monolithic, uniform (spatially homogeneous) value risks misrepresenting the processing capacity of the area of interest and will almost certainly distort the perceived reactive volume of sediment in the hyporheic zone.

Acknowledgments
We appreciate the cooperation of S. Nicol of Idaho State Parks with collecting sand. Bob Basham's help was critical in designing and implementing the flume experiments. Many others, including M. Lytle, C. Beeson, R. Hillsberry, L. Hoaks, M. Patterson, J. Fisher, and R. Will provided assistance in setting up the experiment, collecting samples, and analyzing laboratory samples. *Funding sources*: This work was supported by NSF grants 1141690, 1141752, and IIA-1301792. *Data*: The data that were used in support of these findings have been deposited in Hydroshare (Reeder et al., 2018).

References

Appelo, C. A. J., & Postma, D. (2010). *Geochemistry, groundwater and pollution* (2nd ed.). Boca Raton, FL: CDC Press.

Argerich, A., Haggerty, R., Johnson, S. L., Wondzell, S. M., Dosch, N., Corson-Rikert, H., et al. (2016). Comprehensive multiyear carbon budget of a temperate headwater stream. *Journal of Geophysical Research: Biogeosciences*, *121*, 1306–1315. https://doi.org/10.1002/2015JG003050

Bardini, L., Boano, F., Cardenas, M. B., Revelli, R., & Ridolfi, L. (2012). Nutrient cycling in bedform induced hyporheic zones. *Geochimica et Cosmochimica Acta*, *84*, 47–61. https://doi.org/10.1016/j.gca.2012.01.025

Beaulieu, J. J., Tank, J. L., Hamilton, S. K., Wollheim, W. M., Hall, R. O., Mulholland, P. J., et al. (2011). Nitrous oxide emission from denitrification in stream and river networks. *Proceedings of the National Academy of Sciences of the United States of America*, *108*(1), 214–219. https://doi.org/10.1073/pnas.1011464108

Boano, F., Harvey, J. W., Marion, A., Packman, A. I., Revelli, R., Ridolfi, L., et al. (2014). Hyporheic flow and transport processes: Mechanisms, models, and biogeochemical implications. *Reviews of Geophysics*, *52*, 603–679. https://doi.org/10.1002/2012RG000417

Bott, T. L., Kaplan, L. A., & Kuserk, F. T. (1984). Benthic bacterial biomass supported by streamwater dissolved organic matter. *Microbial Ecology*, *10*(4), 335–344. https://doi.org/10.1007/BF02015558

Briggs, M. A., Lautz, L. K., Hare, D. K., & González-Pinzón, R. (2013). Relating hyporheic fluxes, residence times, and redox-sensitive biogeochemical processes upstream of beaver dams. *Freshwater Science*, *32*(2), 622–641. https://doi.org/10.1899/12-110.1

Budwig, R., & Goodwin, P. (2012). The Center for Ecohydraulics Research Mountain StreamLab—A facility for collaborative research and education. In *Innovations 2012: World innovations in engineering education and research*. Potomac, MD: iNeer.

Cardenas, M. B., Cook, P. L. M., Jiang, H., & Traykovski, P. (2008). Constraining denitrification in permeable wave-influenced marine sediment using linked hydrodynamic and biogeochemical modeling. *Earth and Planetary Science Letters*, *275*(1–2), 127–137. https://doi.org/10.1016/j.epsl.2008.08.016

Cardenas, M. B., & Wilson, J. L. (2007). Exchange across a sediment–water interface with ambient groundwater discharge. *Journal of Hydrology*, *346*(3–4), 69–80. https://doi.org/10.1016/j.jhydrol.2007.08.019

Chapelle, F. H. (1993). *Ground-water microbiology and geochemistry*. New York, NY: John Wiley.

Chapelle, F. H., McMahon, P. B., Dubrovsky, N. M., Fujii, R. F., Oaksford, E. T., & Vroblesky, D. A. (1995). Deducing the distribution of terminal electron-accepting processes in hydrologically diverse groundwater systems. *Water Resources Research*, *31*(2), 359–371. https://doi.org/10.1029/94WR02525

Cleveland, C. C., Nemergut, D. R., Schmidt, S. K., & Townsend, A. R. (2007). Increases in soil respiration following labile carbon additions linked to rapid shifts in soil microbial community composition. *Biogeochemistry*, *82*(3), 229–240. https://doi.org/10.1007/s10533-006-9065-z

Cooper, A. C. (1965). *The effect of transported stream sediments on the survival of sockeye and pink salmon eggs and alevin*. New Westminster, BC, Canada: International Pacific Salmon Fisheries Commission.

Curiel Yuste, J., Baldocchi, D. D., Gershenson, A., Goldstein, A., Misson, L., & Wong, S. (2007). Microbial soil respiration and its dependency on carbon inputs, soil temperature and moisture. *Global Change Biology*, *13*(9), 2018–2035. https://doi.org/10.1111/j.1365-2486.2007.01415.x

Drummond, J. D., Davies-Colley, R. J., Stott, R., Sukias, J. P., Nagels, J. W., Sharp, A., et al. (2014). Retention and remobilization dynamics of fine particles and microorganisms in pastoral streams. *Water Research*, *66*, 459–472. https://doi.org/10.1016/j.watres.2014.08.025

Elliott, A. H., & Brooks, N. H. (1997). Transfer of nonsorbing solutes to a streambed with bed forms: Theory. *Water Resources Research*, *33*(1), 123–136. https://doi.org/10.1029/96WR02784

Fehlman, H. M. (1985). *Resistance components and velocity distributions of open channel flows over bedforms* (169 pp.). Fort Collins, CO: Colorado State University.

Findlay, S. (1995). Importance of surface-subsurface exchange in stream ecosystems: The hyporheic zone. *Limnology and Oceanography*, *40*(1), 159–164. https://doi.org/10.4319/lo.1995.40.1.0159

Fischer, H., Kloep, F., Wilzcek, S., & Pusch, M. T. (2005). A river's liver: Microbial processes within the hyporheic zone of a large lowland river. *Biogeochemistry*, *76*(2), 349–371.

Furukawa, K., Heinzle, E., & Dunn, I. J. (1983). Influence of oxygen on the growth of *Saccharomyces cerevisiae* in continuous culture. *Biotechnology and Bioengineering*, *25*(10), 2293–2317. https://doi.org/10.1002/bit.260251003

González-Pinzón, R., Haggerty, R., & Argerich, A. (2014). Quantifying spatial differences in metabolism in headwater streams. *Freshwater Science*, *33*(3), 798–811. https://doi.org/10.1086/677555

Greig, S. M., Sear, D. A., & Carling, P. A. (2007). A review of factors influencing the availability of dissolved oxygen to incubating salmonid embryos. *Hydrological Processes*, *21*(3), 323–334. https://doi.org/10.1002/hyp.6188

Harrison, D. E. F. (1972). Physiological effects of dissolved oxygen tension and redox potential on growing populations of micro-organisms. *Journal of Applied Chemistry and Biotechnology*, *22*(3), 417–440. https://doi.org/10.1002/jctb.2720220311

Harvey, J. W., Böhlke, J. K., Voytek, M. A., Scott, D., & Tobias, C. R. (2013). Hyporheic zone denitrification: Controls on effective reaction depth and contribution to whole-stream mass balance. *Water Resources Research*, *49*, 6298–6316. https://doi.org/10.1002/wrcr.20492

Harvey, J. W., Drummond, J. D., Martin, R. L., McPhillips, L. E., Packman, A. I., Jerolmack, D. J., et al. (2012). Hydrogeomorphology of the hyporheic zone: Stream solute and fine particle interactions with a dynamic streambed. *Journal of Geophysical Research*, *117*, G00N11. https://doi.org/10.1029/2012JG002043

Henry, S., Bru, D., Stres, B., Hallet, S., & Philippot, L. (2006). Quantitative detection of the nosZ gene, encoding nitrous oxide reductase, and comparison of the abundances of 16S rRNA, narG, nirK, and nosZ genes in soils. *Applied and Environmental Microbiology*, *72*(8), 5181–5189. https://doi.org/10.1128/AEM.00231-06

Hödl, I., Mari, L., Bertuzzo, E., Suweis, S., Besemer, K., Rinaldo, A., et al. (2014). Biophysical controls on cluster dynamics and architectural differentiation of microbial biofilms in contrasting flow environments. *Environmental Microbiology*, *16*(3), 802–812. https://doi.org/10.1111/1462-2920.12205

Hunter, K. S., Wang, Y., & Van Cappellen, P. (1998). Kinetic modeling of microbially-driven redox chemistry of subsurface environments: Coupling transport, microbial metabolism and geochemistry. *Journal of Hydrology*, *209*(1–4), 53–80. https://doi.org/10.1016/S0022-1694(98)00157-7

Kayser, A., Weber, J., Hecht, V., & Rinas, U. (2005). Metabolic flux analysis of Escherichia coli in glucose-limited continuous culture. I. Growth-rate-dependent metabolic efficiency at steady state. *Microbiology*, *151*(3), 693–706. https://doi.org/10.1099/mic.0.27481-0

Kessler, A. J., Glud, R. N., Cardenas, M. B., Larsen, M., Bourke, M. F., & Cook, P. L. M. (2012). Quantifying denitrification in rippled permeable sands through combined flume experiments and modeling. *Limnology and Oceanography*, *57*(4), 1217–1232. https://doi.org/10.4319/lo.2012.57.4.1217

King, S. A., Heffernan, J. B., & Cohen, M. J. (2014). Nutrient flux, uptake, and autotrophic limitation in streams and rivers. *Freshwater Science*, *33*(1), 85–98. https://doi.org/10.1086/674383

Krause, S., Hannah, D. M., Fleckenstein, J. H., Heppell, C. M., Kaeser, D., Pickup, R., et al. (2011). Inter-disciplinary perspectives on processes in the hyporheic zone. *Ecohydrology*, *4*(4), 481–499. https://doi.org/10.1002/eco.176

Laanbroek, H. J., Bodelier, P. L. E., & Gerards, S. (1994). Oxygen consumption kinetics of *Nitrosomonas europaea* and *Nitrobacter hamburgensis* grown in mixed continuous cultures at different oxygen concentrations. *Archives of Microbiology*, *161*(2), 156–162. https://doi.org/10.1007/BF00276477

Marzadri, A., Dee, M. M., Tonina, D., Bellin, A., & Tank, J. L. (2017). Role of surface and subsurface processes in scaling N_2O emissions along riverine networks. *Proceedings of the National Academy of Sciences of the United States of America*, *114*, 4330–4335. https://doi.org/10.1073/pnas.1617454114

Marzadri, A., Tonina, D., & Bellin, A. (2010). A semianalytical three-dimensional process-based model for hyporheic nitrogen dynamics in gravel bed rivers. *Water Resources Research*, *47*, W11518. https://doi.org/10.1029/2011WR010583

Marzadri, A., Tonina, D., & Bellin, A. (2012). Morphodynamic controls on redox conditions and on nitrogen dynamics within the hyporheic zone: Application to gravel bed rivers with alternate-bar morphology. *Journal of Geophysical Research*, *117*, G00N10. https://doi.org/10.1029/2012JG001966

Master, Y., Shavit, U., & Shaviv, A. (2005). Modified isotope pairing technique to study N transformations in polluted aquatic systems: Theory. *Environmental Science & Technology*, *39*(6), 1749–1756. https://doi.org/10.1021/es049086c

Moreno-Vivián, C., Cabello, P., Martínez-Luque, M., Blasco, R., & Castillo, F. (1999). Prokaryotic nitrate reduction: Molecular properties and functional distinction among bacterial nitrate reductases. *Journal of Bacteriology*, *181*(21), 6573–6584.

Naranjo, R. C., Niswonger, R. G., & Davis, C. J. (2015). Mixing effects on nitrogen and oxygen concentrations and the relationship to mean residence time in a hyporheic zone of a riffle-pool sequence. *Water Resources Research*, *51*, 7202–7217. https://doi.org/10.1002/2014WR016593

Nobre, A., Duarte, L., Roseiro, J., & Gírio, F. (2002). A physiological and enzymatic study of *Debaryomyces hansenii* growth on xylose- and oxygen-limited chemostats. *Applied Microbiology and Biotechnology*, *59*(4), 509–516. https://doi.org/10.1007/s00253-002-1050-4

Nogaro, G., Datry, T., Mermillod-Blondin, F., Foulquier, A., & Montuelle, B. (2013). Influence of hyporheic zone characteristics on the structure and activity of microbial assemblages. *Freshwater Biology*, *58*(12), 2567–2583. https://doi.org/10.1111/fwb.12233

Ocampo, C. J., Oldham, C. E., & Sivapalan, M. (2006). Nitrate attenuation in agricultural catchments: Shifting balances between transport and reaction. *Water Resources Research*, *42*, W01408. https://doi.org/10.1029/2004WR003773

Packman, A. L., Salehin, M., & Zaramealla, M. (2004). Hyporheic exchange with gravel beds: Basic hydrodynamic interactions and bedform-induced advective flows. *Journal of Hydraulic Engineering*, *130*(7), 647–656. https://doi.org/10.1061/(ASCE)0733-9429(2004)130:7(647)

Pinay, G., O'Keefe, T. C., Edwards, R. T., & Naiman, R. J. (2009). Nitrate removal in the hyporheic zone of a salmon river in Alaska. *River Research and Applications*, *25*(4), 367–375. https://doi.org/10.1002/rra.1164

Pirt, S. J. (1957). The oxygen requirement of growing cultures of an aerobacter species determined by means of the continuous culture technique. *Microbiology*, *16*(1), 59–75. https://doi.org/10.1099/00221287-16-1-59

Pretty, J. L., Hildrew, A. G., & Trimmer, M. (2006). Nutrient dynamics in relation to surface–subsurface hydrological exchange in a groundwater fed chalk stream. *Journal of Hydrology*, *330*(1–2), 84–100. https://doi.org/10.1016/j.jhydrol.2006.04.013

Quick, A. M., Reeder, W. J., Farrell, T. B., Tonina, D., Feris, K. P., & Benner, S. G. (2016). Controls on nitrous oxide emissions from the hyporheic zones of streams. *Environmental Science & Technology*, *50*(21), 11491–11500. https://doi.org/10.1021/acs.est.6b02680

Ramirez, O. T., & Mutharasan, R. (1990). Cell cycle- and growth phase-dependent variations in size distribution, antibody productivity, and oxygen demand in hybridoma cultures. *Biotechnology and Bioengineering*, *36*(8), 839–848. https://doi.org/10.1002/bit.260360814

Reeder, W. J., Quick, A. M., Farrell, T. B., Benner, S. G., Feris, K. P., & Tonina, D. (2018). *Spatially and temporally distributed, high-resolution dissolved oxygen data for the hyporheic zone of multiple dune-like bedforms*. *HydroShare*. http://dx.doi.org/10.4211/hs.c0f61754a85d41e18618bae5473f34d8

Richardson, D., Felgate, H., Watmough, N., Thomson, A., & Baggs, E. (2009). Mitigating release of the potent greenhouse gas N_2O from the nitrogen cycle—Could enzymic regulation hold the key? *Trends in Biotechnology*, *27*(7), 388–397. https://doi.org/10.1016/j.tibtech.2009.03.009

Rosenberger, R. F., & Kogut, M. (1958). The influence of growth rate and aeration on the respiratory and cytochrome system of a fluorescent pseudomonad grown in continuous culture. *Microbiology*, *19*(2), 228–243. https://doi.org/10.1099/00221287-19-2-228

Rutherford, J., Boyle, J., Elliott, A., Hatherell, T., & Chiu, T. (1995a). Modeling benthic oxygen uptake by pumping. *Journal of Environmental Engineering*, *121*(1), 84–95. https://doi.org/10.1061/(ASCE)0733-9372(1995)121:1(84)

Rutherford, J., Boyle, J. D., Elliot, A. H., Hatherell, T. V. J., & Chiu, T. W. (1995b). Modeling benthic oxygen uptake by pumping. *Journal of Environmental Engineering*, *121*(1), 84–95.

Sinclair, C. G., & Ryder, D. N. (1975). Models for the continuous culture of microorganisms under both oxygen and carbon limiting conditions. *Biotechnology and Bioengineering*, *17*(3), 375–398. https://doi.org/10.1002/bit.260170307

Sobczak, W. V., & Findlay, S. (2002). Variation in bioavailability of dissolved organic carbon among stream hyporheic flowpaths. *Ecology*, *83*(11), 3194–3209. https://doi.org/10.1890/0012-9658(2002)083[3194:VIBODO]2.0.CO;2

Stewart, P. S. (2003). Diffusion in biofilms. *Journal of Bacteriology*, *185*(5), 1485–1491. https://doi.org/10.1128/jb.185.5.1485-1491.2003

Stewart, P. S. (2012). Mini-review: Convection around biofilms. *Biofouling*, *28*(2), 187–198. https://doi.org/10.1080/08927014.2012.662641

Stewart, P. S., Davison, W. M., & Steenbergen, J. N. (2009). Daptomycin rapidly penetrates a *Staphylococcus epidermidis* biofilm. *Antimicrobial Agents and Chemotherapy*, *53*(8), 3505–3507. https://doi.org/10.1128/AAC.01728-08

Suberkropp, K. (1998). Effect of dissolved nutrients on two aquatic hyphomycetes growing on leaf litter. *Mycological Research*, *102*(8), 998–1002. https://doi.org/10.1017/S0953756297005807

Tonina, D., & Buffington, J. M. (2007). Hyporheic exchange in gravel bed rivers with pool-riffle morphology: Laboratory experiments and three dimensional modeling. *Water Resources Research*, *43*, W01421. https://doi.org/1029/2005WR004328

Tonina, D., & Buffington, J. M. (2009). A three-dimensional model for analyzing the effects of salmon redds on hyporheic exchange and egg pocket habitat. *Canadian Journal of Fisheries and Aquatic Sciences*, *66*(12), 2157–2173. https://doi.org/10.1139/F09-146

Tonina, D., & Buffington, J. M. (2011). Effects of stream discharge, alluvial depth and bar amplitude on hyporheic flow in pool-riffle channels. *Water Resources Research*, *47*, W08508. https://doi.org/10.1029/2010WR009140

Triska, F. J., Duff, J. H., & Avanzino, R. J. (1993a). The role of water exchange between a stream channel and its hyporheic zone in nitrogen cycling at the terrestrial-aquatic interface. *Hydrobiologia*, *251*(1–3), 167–184. https://doi.org/10.1007/BF00007177

Triska, F. J., Duff, J. H., & Avanzino, R. J. (1993b). Patterns of hydrological exchange and nutrient transformation in the hyporheic zone of a gravel-bottom stream: Examining terrestrial—aquatic linkages. *Freshwater Biology*, *29*(2), 259–274. https://doi.org/10.1111/j.1365-2427.1993.tb00762.x

Wörman, A., Packman, A. I., Johansson, H., & Jonsson, K. (2002). Effect of flow-induced exchange in hyporheic zones on longitudinal transport of solutes in streams and rivers. *Water Resources Research*, *38*(1), 1001. https://doi.org/10.1029/2001WR000769

Wrage, N., Velthof, G. L., van Beusichem, M. L., & Oenema, O. (2001). Role of nitrifier denitrification in the production of nitrous oxide. *Soil Biology and Biochemistry*, *33*(12–13), 1723–1732. https://doi.org/10.1016/S0038-0717(01)00096-7

Wriedt, G., & Rode, M. (2006). Modelling nitrate transport and turnover in a lowland catchment system. *Journal of Hydrology*, *328*(1–2), 157–176. https://doi.org/10.1016/j.jhydrol.2005.12.017

Wuhrmann, K. (1972). Stream purification. In R. Mitchell (Ed.), *Water pollution microbiology* (pp. 119–151). New York, NY: Wiley-Interscience.

Zarnetske, J. P., Haggerty, R., Wondzell, S. M., & Baker, M. A. (2011a). Labile dissolved organic carbon supply limits hyporheic denitrification. *Journal of Geophysical Research*, *116*, G04036. https://doi.org/10.1029/2011JG001730

Zarnetske, J. P., Haggerty, R., Wondzell, S. M., & Baker, M. A. (2011b). Dynamics of nitrate production and removal as a function of residence time in the hyporheic zone. *Journal of Geophysical Research*, *116*, G01025. https://doi.org/10.1029/2010JG001356

Zarnetske, J. P., Haggerty, R., Wondzell, S. M., Bokil, V. A., & González-Pinzón, R. (2012). Coupled transport and reaction kinetics control the nitrate source-sink function of hyporheic zones. *Water Resources Research*, *48*, W11508. https://doi.org/10.1029/2012WR011894